MirrorVLC: Optimal Mirror Placement for Multi-Element VLC Networks

Sifat Ibne Mushfique, Ahmad Alsharoa *Senior Member, IEEE,*, and Murat Yuksel, *Senior Member, IEEE*

***Abstract*—Visible Light Communication (VLC) is a rapidly growing technology which can supplement the current radio-frequency (RF) based wireless communication systems. VLC can play a huge part in solving the ever-increasing problem of spectrum scarcity because of the growing availability of Light Emitting Diodes (LEDs). One of the biggest advantages of VLC over other communication systems is that it can provide illumination and data communication simultaneously without needing any extra deployment. Although it is essential to provide data rate at a blazing speed to all the users nowadays, maintaining a satisfactory level in the distribution of lighting is also important. In this paper, we present a novel approach of using mirrors to enhance the illumination uniformity and throughput of an indoor multi-element VLC system architecture. In this approach, we improve the Signal-to-Interference plus Noise Ratio (SINR) of the system and overall illumination uniformity of the room by redirecting the reflected LED beams on the walls to darker spots with the use of mirrors. We formulate a joint optimization problem focusing on maximization of the SINR while maintaining a reasonable illumination uniformity across the room. We propose a two-stage solution of the optimization problem: design solution and communication solution. In the design optimization, we formulate an equivalent binary linear optimization to achieve the best illumination quality by optimizing the mirror placements and the LEDs' transmit powers. In the communication problem, however, we aim to improve the throughput of the system using a fair utility metric based on maximizing the minimum user's data rate. Due to non-convexity of the communication problem, we propose three different heuristic solutions and analyze their performance. We also show that about threefold increase in average illumination and fourfold increase in average throughput can be achieved when the mirror placement is applied which is a significant performance improvement.**

***Index Terms*—Visible Light Communication; Illumination Uniformity; Joint Optimization;**

I. Introduction

VISIBLE Light Communications (VLC) is a rapidly unfolding technology with noteworthy potential to meet the necessity of wireless access speeds. With the constantly increasing number of Internet-of-Things (IoT) devices and the humongous demand for wireless bandwidth, VLC solutions are of lofty worth. VLC is considered as one of the promising indoor communication technologies in terms of transceiver convenience and channel characteristics [1]. Most of the related works in VLC have concentrated on diffuse optics [2] and diversity combining [3] for downloading a data stream to devices in a room. At the modulation level, OFDM [4], [5] and Multi-Input Multi-Output (MIMO) [6], [7] techniques were explored to increase the VLC link capacities. Unlike diffuse optics, Multi-element VLC (where multiple transmitters are involved in a VLC system design) allows several LED transmitters with narrow divergence angles to transmit different datastreams simultaneously. Because of this capability, optical wireless communications researchers gained interest in multi-element VLC architectures [8]–[10] in the recent times. The multi-element VLC networks can offer increased aggregate throughput via simultaneous wireless links and attain higher spatial reuse. The downlink data transmission efficiency may be considerably enhanced by using multi-element VLC modules due to its light beam directionality where each transmitter, e.g., a Light Emitting Diode (LED), can be modulated with different data streams. Although, with this, the problem of maintaining a balanced illumination also arises because of the potential creation of dark spots in between the directional beams of the transmitters.

Most of the VLC literature can be categorized into four groups based on the number of transmitters and datastreams involved in the design. *Single Element Single Datastream (SESD)* designs are based on the concept of a single LED transferring a single datastream to a particular receiver. Most of the studies conducted in the early stages of VLC research were based on SESD VLC systems with a focus on improving the SINR [11], [12]. *Single Element Multi Datastream (SEMD)* is another form of VLC design where considerable amount of exploration has been done where a single transmitter is able to serve multiple receivers simultaneously or via time sharing methods like Time Division Multiple Access (TDMA) [13], [14] - most of these techniques involved diffuse optics. Apart from these two designs, other two can be categorized in multi-element VLC. *Multi Element Single Datastream (MESD)* design allows multiple LEDs to send data towards one receiver which increases the received light intensity at it. Usage of more than one transmitter allows MESD to employ cooperative transmission [15] to reduce Bit Error Rate (BER) and also various MIMO techniques by placing multiple photo-detectors at the receiver end where such demonstrated an improvement in data rate [16]. Despite having these benefits, MESD VLC designs cannot afford high directionality when transferring different data streams to different receiver at the same time, which is possible in *Multi Element Multi Datastream (MEMD)*. These designs have surfaced in recent times, and various combinations in LED positioning are possible in these designs

Sifat Ibne Mushfique (sifat.im@knights.ucf.edu) and Murat Yuksel (murat.yuksel@ucf.edu) are with University of Central Florida (UCF), Orlando, Florida, USA. Ahmad Alsharoa (aalsharoa@mst.edu) is with Missouri University of Science and Technology (MST), Rolla, Missouri, USA.

due to the flexibility in the number of elements and datastreams. Our proposed design is under MEMD category where the advantage of light beam directionality is utilized in multi-element VLC system. More details on this categorization can be found in one of our earlier works [17].

Illumination uniformity is a critical element to be examined in a multi-element VLC architecture where uniform light distribution is essential to be maintained as each LED's transmit power is being tuned. Otherwise, inconsistent lighting might appear while the transmit powers of LEDs are being tuned for maximal SINR. Thus, it is important to ensure uniform lighting in the room, while optimizing for the LED assignment problem with a source power constraint on each LED. This type of multi-element architecture can improve the system performance in terms of SINR as investigated in [18], [19]. In our prior work [17], we showed that tradeoffs between uniform lighting and high SINR in MEMD VLC networks can be explored in a practical manner. Our work in this paper uses a different approach from the previous works in the literature, where we explore a novel approach of using mirror placement in MEMD VLC networks with narrow-angle LEDs in order to use the non-line-of-sight (NLoS) light beams for improving overall throughput and the evenness of lighting. We propose a novel MEMD VLC framework design with a hemispherical shaped multi-element bulb containing multiple LEDs and several mirrors mounted in the walls. This hemispherical shape allows high spatial reuse in addition to improving the illumination uniformity of the room. Light is emitted in different directions from the LEDs, and hence, the spherical multi-element bulb helps attaining an evenly scattered lighting. We further improve the average SINR and illumination uniformity of the system by formulating and solving an optimization problem, which optimizes the number of the mirrors as well as source power and assignment of the LEDs to the users to improve system performance. Apart from the multi-element hemispherical bulb optimization, we introduce optimizing the placement of multiple mirrors at rooms' walls for a better illumination and communications performance. We formulated and solved a joint optimization of the LEDs' transmit power and association with receivers to improve the aggregate data rate (of multiple data streams) and illumination uniformity in multi-element VLC networks. To the best of authors' knowledge, this paper proposes for the first time the placement optimization of multiple mirrors jointly with LEDs' power and associations. The main contributions are as follows:

- Investigating a hemispherical multi-element bulb architecture in downlink VLC transmission, where each LED can be assigned to a receiver to contribute towards data transmission or towards uniform illumination. The following assumptions are used: i) the transmission times of all LEDs are synchronized, ii) all consecutive symbols arriving to a certain user are aggregated with neglected delays, and iii) the interference signals coming from a group of LEDs serving to different users are assumed to add up linearly.
- Introducing a mirror placement approach that maximizes the ratio of SINR over the illumination uniformity of the system by formulating it as an optimization problem. The proposed approach has shown three-fold improvement in throughput and four-fold improvement in illumination quality compared to the case when there is no mirror in the wall.
- Proposing multiple ways to place mirrors across the room walls, comparing and analyzing their performance with respect to the case of without any mirror placement.
- Proposing a two-stage solution of the optimization problem to avoid the impracticality of changing mirror locations based on changes in the position of mobile users: (1) design problem: we propose a binary linear optimization problem with the goal of achieving the best illumination quality by optimizing the mirror placements and the LEDs' transmit powers, and (2) communication problem: due to the non-convexity of the problem, we propose multiple low complexity heuristic algorithms to achieve efficient solutions that focus on maximizing the throughput of the system.
- Analyzing the system performance under imperfect VLC channel information scenario.
- Extensive simulation results illustrating the advantages of our proposed model. The results show that the system without mirror placement optimization suffers from low illumination and low average throughput compared to the mirror optimization case. In a typical scenario with 3 or more users in the room, adding mirrors to the design can improve the average throughput 10 times while also improving the average illumination by 3 times. The results also show the trade-off of the LEDs' divergence angles on receivers coverage and interference. With larger divergence angles, the LED beams get larger, which leads to more chances of a receiver to get covered under one or more LEDs. However, because each LED can be assigned to difference receivers at the same time, the receivers will also get more chances of interference.

The rest of the paper is organized as follows: Section II describes our spherical multi-element VLC architecture and the overall system model. The formulation of the proposed joint optimization problem along with the details of the two-stage solution is presented in Section III. Selected numerical simulation results are presented in Section IV. Finally, we survey the related work in Section V and summarize our work in Section VI.

II. System Model

We consider a VLC downlink system model in an indoor setting consisting of a single hemispherical bulb containing M directional LED transmitters in L layers to serve U mobile users. The transmit power of each LED is P_m Watt, $\forall m = 1, .., M$ as shown in Fig. 1. Table I summarizes the notations and symbols we will use in building the rest of of the system model. The bulb is a hemispherical structure with two goals: i) achieve uniform lighting illumination within the room, and ii) provide high speed wireless download to mobile users. We assume that the LEDs in the bulb are placed in different layers in order to cover different locations in the room.

TABLE I: Table of Symbols

Symbol	Meaning
$h_{ml}^{\text{LoS}}/h_{ml}^{\text{NLoS}}$	LoS/NLoS channel model between LED m and node l
H_{ml}	total channel model between LED m and node l
$\hat{H}_{ml}$	estimated CSI channel
ΔH_{ml}	CSI errors corresponding to the estimated CSI channel
σ_e^2	variance of the estimated CSI channel error, ΔH_{ml}, with a complex Gaussian distribution
A_l	receiver l node's PD area
d_{ml}	distance between LED m and node l
φ_{ml}/ϕ_{ml}	irradiance/incidence angles
$Q_0(\varphi_{ml})$	Lambertian radiant intensity
q	order of Lambertian emission
Υ_{zm}	set of z indices corresponding to the reflection area of LED m
χ_{mz}	binary variable that expresses whether or not a NLoS component from LED m via grid location z
ϑ	illumination uniformity
ϵ_{mu}	Binary variable indicates if LED m is associated with user u
P_m	LED m power transmission
y_u	received signal at user u
$s_m(t)$	top of the background DC light intensity
μ	minimum acceptable illumination uniformity for an indoor setting

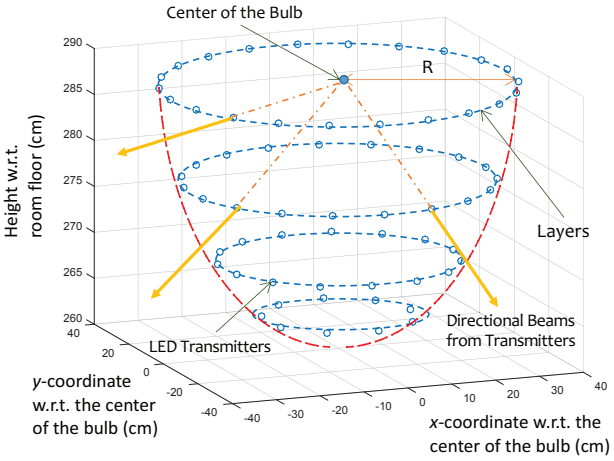

Fig. 1: Placement of transmitters in the multi-element bulb with 4 layers.

In order to improve the illumination uniformity and download speed to mobile users, we consider placing mirrors to the walls into the room's wall aiming to utilize NLoS beams from the LEDs. We divide each wall into an $X \times Y$ grid. We assume that in each grid element, one mirror can be placed at most. We call this mirror as a 'grid mirror'. We anticipate that these grid mirrors in the walls will reflect the NLoS signals and thus potentially enhance the performance of the multi-element VLC network. The optimal placement of the mirrors, among other factors, will depend on the direction of the incident lights from the LEDs to the walls. We consider that a user's photo-detector (PD) gain depends on the light intensity from three main directions: 1) the LoS beams directly coming from LEDs, 2) strong reflections of the LoS light beams from the grid mirrors, and 3) weak-reflected light from the regular walls as shown in Fig 2. Since there are four walls and each one is divided as $X \times Y$ sized grid, we visualize the scope of mirror

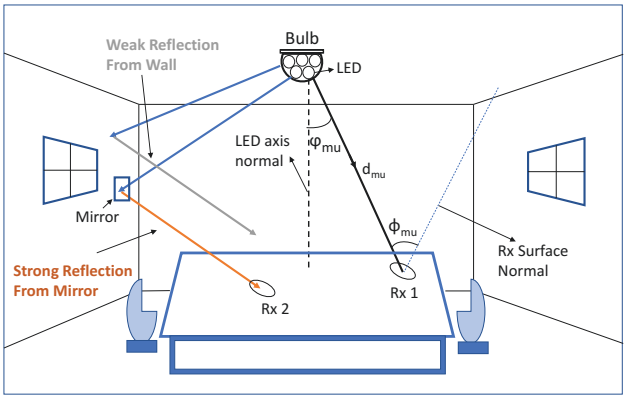

Fig. 2: System Model.

placement as a $4X \times Y$ grid, where four walls are assumed to be placed side-by-side. Each cell of the grid can be defined with index z where $z = 1, 2, 3, ...Z$, here $Z = 4XY$.

To compute the illumination uniformity in our simulated environment, we consider $n = 1, 2, 3, ...N$ fixed sensing points uniformly distributed inside the room. The light intensity received at these points determine how uniform the lighting is inside the room. Although any of them can be placed at a place of interest, we assume that they are uniformly distributed to the room floor in a lattice placement pattern.

We also consider that each mobile user is equipped with a single PD to receive the downlink light beams. It is assumed that the location of the mobile users in the room can be predicted. On the other hand, we assume that the mobile users are equipped with an RF transmitter such as Wi-Fi for uplink transmission. In this work, we focus on downlink transmissions only and assume that the uplink transmission speed is not a bottleneck which is also the case for typical wireless access at an indoor setting.

A. VLC Channel Model

1) LoS Channel: The LoS channel model between LED m and receiver node l ($l \in \{u$ for users, n for sensing points$\}$) can be expressed as [20]:

$$h_{ml}^{\text{LoS}} = \begin{cases} \frac{A_l}{d_{ml}^2} Q_0(\varphi_{ml}) \cos(\phi_{ml}) & , \ 0 \le \phi_{ml} \le \phi_c \\ 0 & , \ \phi_{ml} \ge \phi_c \end{cases} \quad (1)$$

where A_l is the receiver node's PD area and d_{ml} is the distance between LED m and node l. φ_{ml} and ϕ_{ml} are the irradiance and incidence angles, respectively, as shown in Fig. 2. ϕ_c is the FOV angle of the PD. We have assumed that no optical filter is used. $Q_0(\varphi_{ml})$ is the Lambertian radiant intensity and expressed as

$$Q_0(\varphi_{ml}) = \frac{(q+1)}{2\pi} \cos^q(\varphi_{ml}), \quad (2)$$

where $q = -\ln(2)/\ln(\cos(\varphi_{1/2}))$ is the order of Lambertian emission and $\varphi_{1/2}$ is the transmitter semi-angle at half power.

2) NLoS Channel: For simplicity, we consider only the strong reflections of the LoS light beams for computing the NLoS channel model. In a scenario where the light from LED

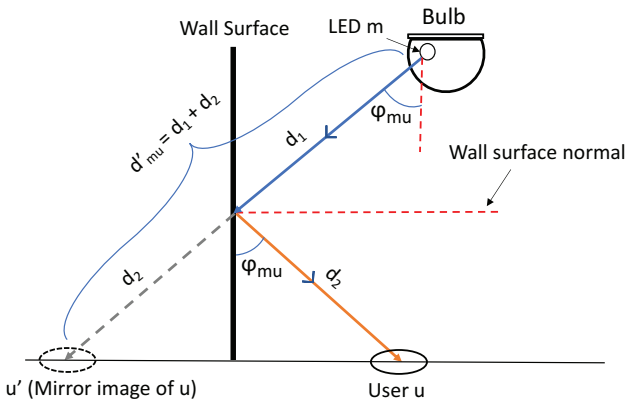

Fig. 3: Comparison between an NLoS channel with mirror and LoS channel by using a mirror image of user u to the wall from the same LED m.

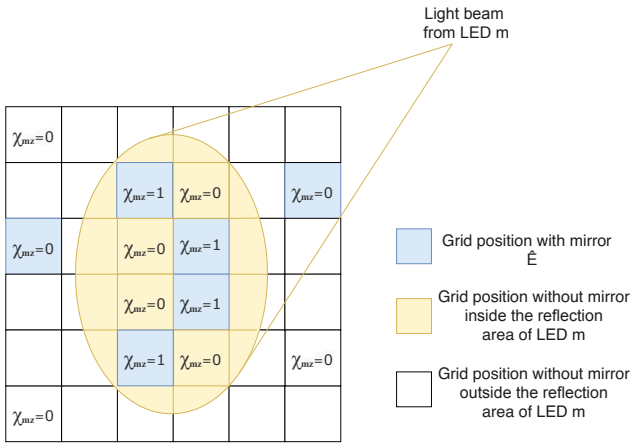

Fig. 4: Figure explaining different values of χ_{mz} in a room wall. $\chi_{mz} = \xi_z$ when grid position z is inside the reflection area of LED m (marked in orange) and 0 otherwise. Grid positions with mirrors are marked in light blue.

m is coming to user u through a grid mirror located at ξ_z (i.e., $\xi_z = 1$), the NLoS channel model between LED m and node l can be expressed as [21]:

$$h_{ml}^{\text{NLoS}}(z) = \frac{\eta A_l}{\hat{d}_{ml}(z)^2} Q_0(\varphi_{ml}) \cos(\phi_{ml}) \tag{3}$$

where η is the reflection coefficient of a grid mirror and $\hat{d}_{ml}(z)$ is the distance between m and l via the mirror located at index z of the grid ξ. This is explained in Fig. 3 where we compare the NLoS channel between LED m and user u with a channel between m and u' which is a mirror image of u with respect to the wall. We can see that the distance between m and u' is same as the total distance between m and u via the mirror. Therefore, we can express the NLoS channel between m and u as the LoS channel between m and u' with the following in consideration - the NLoS channel strength will be reduced by a factor as there is a mirror in its path, and this factor is dependent on η, the reflection coefficient of the mirror. Same expression can be derived for the sensing points as well, thus we present the general expression for node l in (3). As discussed in [21], the reflection coefficient is between 0 and 1 depending on mirrors' reflectivity, and can reach $\eta = 0.99$ for high-reflection coating mirrors, which we used in our evaluations.

3) Total Channel: We can express the total channel model as the combination of LoS and NLoS channels. By considering an imperfect Channel State Information (CSI) scenario, the channel can be modeled as follows:

$$\begin{aligned} H_{ml}(\xi_z, \chi_{mz}, \Delta H_{ml}) &= \hat{H}_{ml} + \Delta H_{ml} \\ &= \left(h_{ml}^{\text{LoS}} + \sum_{z=1}^{Z} \chi_{mz} h_{ml}^{\text{NLoS}}(z) \right) + \Delta H_{ml}, \end{aligned} \tag{4}$$

such that

$$\begin{aligned} \chi_{mz} &= \xi_z, & if \;\; z \in \Upsilon_{zm}, \\ \chi_{mz} &= 0, & \text{otherwise}, \end{aligned} \tag{5}$$

where $\hat{H}_{ml}$ is the estimated CSI channel, and ΔH_{ml} is the corresponding CSI errors. We assume that the estimated CSI channel errors, ΔH_{ml}, are independent and identically distributed with zero mean complex Gaussian and variances σ_e^2 [22]–[24]. The estimated and real channels are equal when $\sigma_e^2 = 0$, which is denoted as perfect CSI scenario. VLC channels are mostly stable in indoor environments, particularly at short ranges. Taking a precautionary approach, the channel model above considers the imperfect CSI for completeness. Hence, the CSI estimation error σ_e is mostly going to be close to zero in practice.

To explain the above channel clearly, we define *reflection area* of LED m as the wall area being covered by the beam coming from LED m. The parameter Υ_{zm} given in (5) is the set of z indices corresponding to the reflection area of LED m. $\xi_z = 1$ if a grid mirror is placed at the cell located at index z of the grid ξ and $\xi_z = 0$ otherwise. Further, χ_{mz} is a binary variable that expresses whether or not a NLoS component from LED m via grid location z will be accumulated in the channel. Note that χ_{mz} cannot be 1 if the grid location z is not within the reflection area of LED m. However, if the grid location z is within the reflection area of LED m, then it can be 0 or 1 depending on the existence of a grid mirror at z which is expressed by ξ_z. Fig. 4 explains different values for χ_{mz}. Although the above explained model seems a bit complex primarily because of the inclusion of an extra dependent variable χ_{mz}, a designer of a VLC system can enjoy much more flexibility because of this. By bringing different combinations of χ_{mz} into the overall search space, probability of finding a near optimal solution becomes much higher as we can control the contribution of every small fractions of each LED beam to either illumination only, or both illumination and communication.

B. Illumination Uniformity

The illumination intensity distribution across the room is an important factor to be considered in VLC system. One of common metric to measure the illumination intensity is the illumination uniformity. The illumination uniformity, ϑ, can be defined as the ratio between the minimum and the average

illumination intensity among all N sensing points and is given as [25]:

$$\vartheta = \frac{\min\limits_{n\in\{1,2,..,N\}} \left(\sum\limits_{m=1}^{M} \alpha_0 P_m H_{mn}(\xi_z, \chi_{mz}, \Delta H_{mn}) \right)}{\frac{1}{N} \sum\limits_{n=1}^{N} \sum\limits_{m=1}^{M} \alpha_0 P_m H_{mn}(\xi_z, \chi_{mz}, \Delta H_{mn})} \quad (6)$$

where α_0 is the luminous efficiency that depends on the LED color wavelength, e.g. $\alpha_0 = 60$ lumen/watt for white LED [26]. Note that $\min(.)$ denotes the minimum function.

C. LED-User Association

We use a binary variable ϵ that indicates the association between LED m and user u which is given as follows:

$$\epsilon_{mu} = \begin{cases} 1, \text{if LED } m \text{ is associated with user } u. \\ 0, \text{otherwise.} \end{cases} \quad (7)$$

We assume that user u can be associated with multiple LEDs at the same time. However, it is assumed that each LED can be associated with one user at most during the same time. Even in the case where multiple users are inside the coverage of an LED, it is assigned to only one user. The signal from this LED is treated as interference to the other users in coverage which are not associated with it. Therefore, the following conditions should be respected:

$$\sum_{u=1}^{U} \epsilon_{mu} \leq 1, \forall m = 1, .., M. \quad (8)$$

D. SINR Calculation

For the SINR calculations, we consider the communication signal for the LED m to be carried on the background DC light intensity with a certain amount of power. The transmit power P_m is equal to DC power when the LED is providing illumination only, and equal to the average power when providing both illumination and communication. We assume that each LED is either associated with one user or used for lighting only. Thus, the received signal at user u is given by:

$$y_u = \underbrace{\sum_{m=1}^{M} \epsilon_{mu} P_m H_{mu} s_m}_{\text{signal term}} + \underbrace{\sum_{\substack{k=1 \\ k\neq u}}^{U} \sum_{m=1}^{M} \epsilon_{mk} P_m H_{mk} s_m}_{\text{interference term}} + \underbrace{n_u}_{\text{noise term}} \quad (9)$$

where n_u is the additive Gaussian noise (AWGN) at user u. Following the model in [27], we assume that (i) all LEDs have equal background DC light intensity, (ii) the communication signal from the LED m is a zero-mean signal $s_m(t)$ that is superposed on top of the background DC light intensity, and has AC power $p_m = \text{var}(s_m(t))$ with the standard deviation $P_m = \sqrt{p_m} = \text{std}(s_m(t))$ which we use to calculate the received power, and (iii) all P_ms can be tuned individually and limited by P_{min} and $\bar{P}$ as follows: $P_{min} \leq P_m \leq \bar{P}$. Therefore, SINR at user u can be expressed as [27]

$$\begin{aligned} \Gamma_u &= \frac{\left(\sum\limits_{m=1}^{M} \epsilon_{mu} \hat{H}_{mu}(\xi_z, \chi_{mz}, \Delta H_{mu}) P_m \right)^2}{N_0 B + \sum\limits_{\substack{k=1 \\ k\neq u}}^{U} \left(\sum\limits_{m=1}^{M} \epsilon_{mk} \hat{H}_{mk} P_m(\xi_z, \chi_{mz}, \Delta H_{mk}) \right)^2} \\ &= \frac{\left(\sum\limits_{m=1}^{M} \epsilon_{mu} \hat{H}_{mu} P_m \right)^2}{N_0 B + \sum\limits_{\substack{k=1 \\ k\neq u}}^{U} \left(\sum\limits_{m=1}^{M} \epsilon_{mk} \hat{H}_{mk} P_m \right)^2 + \sigma_e^2} \end{aligned} \quad (10)$$

where B and N_0 are the communication bandwidth and the spectral density of the AWGN, respectively. The received signal strength at u, shown in the numerator, is the sum of all signals from LEDs associated to u as well as their reflections from mirrors. The expression in the numerator constructively adds the received signals from all LEDs (either directly or indirectly as reflection from mirrors) that are assigned to u. However, the signals from all other LEDs and their reflections arriving at u are considered destructive and factored in as interference in the denominator. In the SINR expression above, we followed the assumptions in [27]: i) the transmission times of all LEDs are synchronized, ii) all consecutive symbols arriving to a certain user are aggregated with neglected delays, and iii) the interference signals coming from a group of LEDs serving to different users are assumed to add up linearly.

III. Problem Formulation and Solution

In a nutshell, we propose an optimization problem to optimize the combination of SINR and illumination uniformity based on mirror placement on the wall (ξ_z), LED-user assignment (ϵ_{mu}) and source power for each of the m LEDs (P_m). Although it is possible to re-optimize the objective value by updating ϵ_{mu} whenever a user changes its position, it is not feasible to do so for the mirrors. For this reason, we have divided the problem in two separate optimization problems. First, we find the optimal mirror placements and LED source powers that maximize the illumination uniformity, and then, we optimize the LED-user association along with tuning the LED source powers to maximize the combination of SINR and illumination uniformity using the results from the first problem. This staging makes the optimal mirror placement more practical. In particular, the solution to the first problem will yield the best places to set up the grid mirrors so that high illumination uniformity is attained. Then, the second problem can be solved on-the-fly as users are moving in the room, yielding the best LED transmit powers and LED-user association depending on the user movements.

In this section we formulate two optimization problems defined as mirror design problem and communication problem.

A. Design Problem

The main goal of this problem is to achieve the best illumination quality by optimizing not only the mirror placements

but also the LEDs' transmit powers. Achieving best uniform illumination can be done by maximizing the minimum received power to the ground sensors while considering maximum and minimum illumination levels. Therefore, the mirror design optimization can be formulated as follows:

MIRROR_DESIGN :

$$\underset{\xi_z,\chi_{mz},P_m}{\text{maximize}} \min_{n} \left(\sum_{m=1}^{M} \alpha_0 P_m H_{mn}(\xi_z, \chi_{mz}, \Delta H_{mn}) \right) \quad (11)$$

subject to (5) and

$$P_{min} \leq P_m \leq \bar{P}, \ \ \forall m, \quad (12)$$

$$\vartheta \geq \mu, \quad (13)$$

$$\phi_2 \leq \sum_{m=1}^{M} \alpha_0 P_m H_{mn}(\xi_z, \chi_{mz}, \Delta H_{mn}) \leq \phi_1, \ \ \forall n, \quad (14)$$

$$\chi_{mz} \in \{0,1\}, \ \ n \in \{1,2,..,N\} \quad (15)$$

where P_{min} and $\bar{P}$ are the minimum and maximum source power respectively that can be allotted to an LED and μ is the minimum acceptable illumination uniformity for an indoor setting [25]. χ_{mz} is a dependent variable here, i.e., it is directly related to the values of ξ_z. ϕ_1 and ϕ_2 are the maximum and minimum levels of total illumination allowed at a particular sensing point. These are introduced to ensure that the room is illuminated at a minimum level and also it does not go beyond a level where it can be harmful to human eye.

We aim to solve the above design optimization problem, MIRROR_DESIGN, optimally. In order to do this, we first revise the objective function (11) and constraint (14) by introducing a new decision variable ϕ as follows [28]:

$$\phi = \min_{n} \sum_{m=1}^{M} \alpha_0 P_m \underbrace{\left(h_{mn}^{\text{LoS}} + \sum_{z=1}^{Z} \chi_{mz} h_{mn}^{\text{NLoS}}(z) + \Delta H_{mn} \right)}_{H_{mn}(\xi_z, \chi_{mz})} \quad (16)$$

where $n \in \{1,2,..,N\}$. In (16), $H_{mn}(\xi_z, \chi_{mz})$ is expanded as expressed in (4). (16) is a non-linear equation because of the multiplication between the binary variable χ_{mz} and the real variable P_m. To linearize (16) (i.e., eliminating the products of χ_{mz} and P_m from the problem) we introduce a new decision variable, ρ_{mz}, as $\rho_{mz} = \chi_{mz} P_m$. As such, (16) can be re-written as follows:

$$\phi = \min_{n \in \{1,2,..,N\}} \left(\sum_{m=1}^{M} \alpha_0 P_m h_{mn}^{\text{LoS}} + \sum_{z=1}^{Z} \alpha_0 \rho_{mz} h_{mn}^{\text{NLoS}}(z) + \alpha_0 P_m \Delta H_{mn} \right).$$

As shown in the sequel, after replacing $\chi_{mz} P_m$ with ρ_{mz}, the optimization can be written as a mixed integer linear problem.

Indeed maximizing the objective function given in (11) is equivalent to maximizing ϕ given that $\phi \leq \sum_{m=1}^{M} \alpha_0 P_m H_{mn}$, $\forall n$. Introducing ρ_{mz} can linearize the optimization problem, however, it is needed to replace $\rho_{mz} = \chi_{mz} P_m$ with linear equivalency. Therefore, the following inequalities must be respected [29], [30]:

$$\begin{aligned} &1) \quad P_m \geq \rho_{mz} \geq 0, \forall m, \forall z \\ &2) \quad \rho_{mz} \geq \bar{P}_m \chi_{mz} - \bar{P}_m + P_m, \forall m, \forall z \\ &3) \quad \rho_{mz} \leq \bar{P}_m \chi_{mz}, \forall m, \forall z. \end{aligned} \quad (17)$$

The first two inequalities ensure that ρ_{mz} value is between χ_{mz} and P_m. The third inequality guarantees that $\rho_{mz} = 0$ if $\chi_{mz} = 0$, and $\rho_{mz} = P_m$ if $\chi_{mz} = 1$. By linearizing the MIRROR_DESIGN, the problem is transformed into a mixed-integer linear programming problem. Therefore, the optimization problem can be reformulated as binary linear optimization problem as follows:

LINEARIZED_MIRROR_DESIGN :

$$\underset{\substack{\xi_z,\chi_{mz},P_m \\ \phi,\rho_{mz}}}{\text{maximize}} \quad \phi \quad (18)$$

subject to (5), (12), (17), and

$$\phi \geq \frac{\mu}{N} \sum_{n=1}^{N} \sum_{m=1}^{M} \alpha_0 (P_m h_{mn}^{\text{LoS}} + \sum_{z=1}^{Z} \rho_{mz} h_{mn}^{\text{NLoS}}(z) + P_m \Delta H_{mn}), \quad (19)$$

$$\phi \leq \sum_{m=1}^{M} \alpha_0 (P_m h_{mn}^{\text{LoS}} + \sum_{z=1}^{Z} \rho_{mz} h_{mn}^{\text{NLoS}}(z) + P_m \Delta H_{mn}), \forall n. \quad (20)$$

$$\phi_2 \leq \left(\alpha_0 P_m \Delta H_{mn} + \sum_{m=1}^{M} \alpha_0 P_m h_{mn}^{\text{LoS}} + \sum_{z=1}^{Z} \alpha_0 \rho_{mz} h_{mn}^{\text{NLoS}}(z) \right) \leq \phi_1, \quad \forall n, \quad (21)$$

The constraints (19) and (20) are equivalent to constraint (13). The LINEARIZED_MIRROR_DESIGN problem in (18)-(20) is a non-convex mixed-integer linear optimization problem with binary and real variables. The optimal solution for such problems can be found using off-the-shelf software such as Gurobi with CVX interface [31], [32], which, in addition to convex optimization problems, can solve a special case of non-convex optimization problems, i.e., mixed-integer linear problems. Hence, the transformation of the non-convex problem MIRROR_DESIGN to LINEARIZED_MIRROR_DESIGN allows us to use Gurobi with CVX interface.

B. Communication Problem

After solving the mirror placement design optimization problem, we focus now on solving the communication phase aiming to maximize the SINR of the system to ensure the best possible data rate to the users. We choose to use Max-Min utility of the SINR. The approach of maximizing the total data rate which is known in the literature as Max C/I [33], promotes users with favorable channel and interference conditions by allocating them most of the resources, whereas users suffering from higher propagation losses and/or interference levels will have very low data rates. Therefore, due to the unfairness of

total sum data rate utility, the need for more fair utility metrics arises. Following a strict form of fairness, maximizing the ratio of minimum to maximum SINR (or data rate) was used in the literature [34]. Similarly, the Max-Min utilities are a family of utility functions attempting to maximize the minimum SINR in a network [35]. Our goal is to induce more fairness in the network by increasing the priority of users having lower SINR using the Max-Min utility. Thus, we formulate an optimization problem aiming to maximize the minimum SINR of all users by taking the association and illumination intensity constraints into consideration, and express it as

$$\text{MAXMIN\_THROUGHPUT}: \quad \underset{\epsilon_{mu}\in\{0,1\}, P_m \geq 0}{\text{maximize}} \quad \Gamma_{min} \qquad (22)$$
$$\text{subject to (8), (12) and (13),}$$

where $\Gamma_{min} = \min_{u\in\{1,2,..,U\}}(\Gamma_u)$ is the minimum SINR among all users. Note that optimizing ϵ_{mu} and P_m in (22) can avoid destructive signals from the LEDs in order to maximize the SINR.

1) NP Completeness: As the number of LEDs M being considered can be quite large, the number of ways to assign these LEDs to multiple users can be very large and it is practically infeasible to obtain an optimal solution as the users might move frequently inside the room, and the problem is needed to be solved again whenever any of the user coordinates is updated. In fact, this LED assignment problem in consideration is proven to be NP-Complete as elaborated in one of our earlier works [17], so we propose three low complexity heuristic solutions to solve it.

2) Heuristic Approaches: We describe each of our proposed heuristic approaches in this subsection. These heuristics cannot guarantee a globally optimal solution but offer very good results in polynomial time. As users move around in the room, the heuristic will need to be rerun to compute the new LED-user associations and the datastreams (to be downloaded to the users) will be switched among the LEDs accordingly. Hence, it is critical to design heuristics with low computational complexity so that it will be easy to rerun them as the users move around.

Nearest User Assignment (NUA): We denote the resulting P_m values from the solution of LINEARIZED_MIRROR_DESIGN as intermediate power values P_1^{prev}, P_2^{prev}, ... P_M^{prev} for M LEDs, and assign LED m to the closest user to its beam projection if the user lies in the cone of LED m. If there is one or no user in the cone, then we allocate $\min(P_m^{prev}(1+\tau), \bar{P})$ where τ is a measurement of how much we can deviate the allocated power to LED m from its intermediate value P_m^{prev}. We use 0.1 as the value for τ in our simulations. If there is more than one user in the cone of LED m, then we assign this LED to the user which is nearest to the center of the cone of the LED, but with fractional power, since there will be interference in this case as shown in Fig. 5. More details on this heuristic algorithm can be found in [17] where it was introduced for the first time. A detailed pseudo-code of NUA is provided in Algo. 1.

Strongest Signal-based Assignment with User-first Approach (SSA-User): An LED-by-LED assignment approach is implemented in the *NUA* algorithm. In contrast, in this approach, we do a user-by-user assignment. We inspect each user one by one and check the user in consideration is under how many LED beams, either via LoS or via NLoS. There are three possible scenarios -

1) If there is no incoming LED beam towards this user, then we do not assign any LED to it.

2) If there is only one incoming LED beam, then we follow similar approach to *NUA* and assign the user with source power $\min(P_m^{prev}(1+\tau), \bar{P})$.

3) If there are more than one incoming LED beams, then we take total channel model values between each of these LEDs and this particular user into consideration. There are

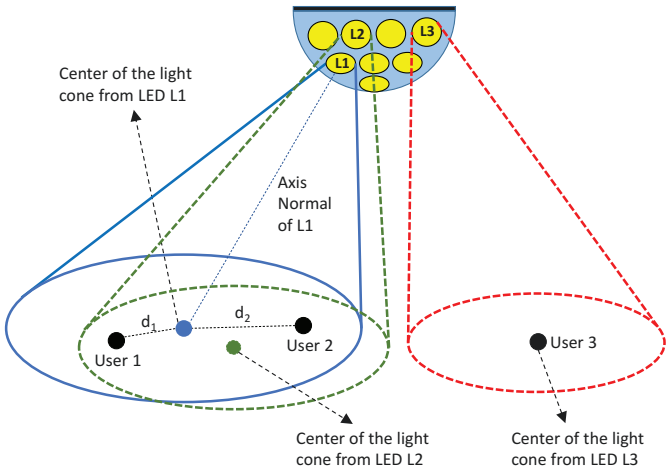

Fig. 5: A case of interference for an user-by-user approach such as *NUA* or *SSA-LED*: LEDs L1, L2 and L3 are assigned to user 1, 2 and 3 respectively. In this case, received power from L2 and L3 will be considered as interference at user 1 - since these LEDs are assigned to user 2 and user 3.

Algorithm 1 Pseudo-code for *NUA* Heuristic Approach

$\boldsymbol{M} \leftarrow$ number of LEDs, $\boldsymbol{U} \leftarrow$ number of users
$\boldsymbol{P_1^{prev}}$, $\boldsymbol{P_2^{prev}}$, ... $\boldsymbol{P_M^{prev}} \leftarrow$ Allocated power to the LEDs from the LINEARIZED_MIRROR_DESIGN solution
$\boldsymbol{\tau} \leftarrow$ Allowed deviation from intermediate value of allocated LED power
for $\boldsymbol{i}$ = 1 to $\boldsymbol{M}$ **do**
  $\boldsymbol{cnt} \leftarrow$ Number of users in the cone of LED $\boldsymbol{i}$
  if $\boldsymbol{cnt} \leq 1$ **then**
    if $\boldsymbol{cnt} == 1$ **then**
      Set $\boldsymbol{\epsilon_{ij}} \leftarrow 1$ $\{\boldsymbol{j}$ is the only user in the cone of LED $\boldsymbol{i}\}$
    end if
    Set $\boldsymbol{P_i} \leftarrow \min(\boldsymbol{P_i^{prev}} + \boldsymbol{\tau}, \bar{\boldsymbol{P}})$
  else
    $\boldsymbol{u_1} \leftarrow$ Nearest user from center of the cone of LED $\boldsymbol{i}$
    $\boldsymbol{d_1} \leftarrow$ Distance of $\boldsymbol{u_1}$ from center of the cone of LED $\boldsymbol{i}$
    $\boldsymbol{u_2} \leftarrow$ Second nearest user from center of the cone of LED $\boldsymbol{i}$
    $\boldsymbol{d_2} \leftarrow$ Distance of $\boldsymbol{u_2}$ from center of the cone of LED $\boldsymbol{i}$
    Set $\boldsymbol{\epsilon_{iu_1}} \leftarrow 1$
    Set $\boldsymbol{P_i} \leftarrow (1 - \boldsymbol{d_1}/\boldsymbol{d_2})\bar{\boldsymbol{P}}$
  end if
end for

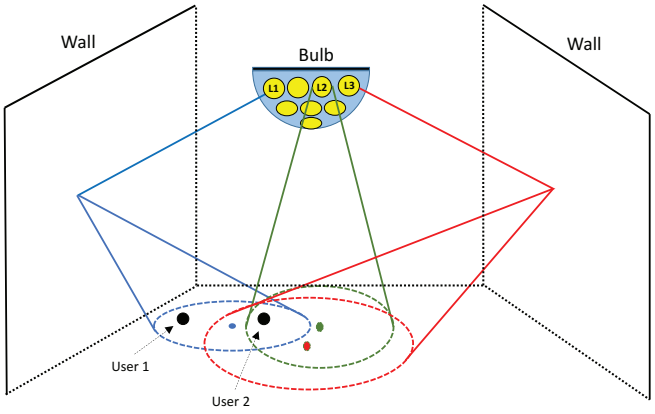

Fig. 6: A case of conflict for an user-by-user approach such as *SSA-User*: both User 1 and User 2 are getting strongest signal from LED L1, but since L1 is assigned to User 1 first, User 2 has to be assigned to L2, which provides the second strongest signal for User 2.

two possible cases in this scenario - i) There is no incoming LED which is already assigned to another user, which means no possible interference - and ii) There is one or more LED(s) which are already assigned to other user(s), which creates interference. In the first case, since there is no chance of interference from any other user, we assign all the incoming LEDs to the user in consideration. However, a much more careful approach is needed for the second case, which is shown in Fig. 6. Here we assign all the incoming LED beams, or simply 'incoming LEDs', to the current user which are not already assigned to other user(s). We calculate the fraction, κ, as the ratio of maximum channel value of all the incoming LEDs including those also which are already assigned to other user(s) denoted as $H_{m_j u_i}$ assuming m_j is the one among these LEDs with strongest channel value with the current user u_i - and maximum of the channel values between all the incoming LEDs to the current user which are still unassigned, denoted as $H_{m_i u_i}$ assuming m_i is the one among these LEDs with strongest channel value with u_i. It can be expressed as $\kappa = \frac{H_{m_j u_i}}{H_{m_i u_i}}$. Finally, we allot the LED m_i with the source power of $\max(P_m^{prev}(1-\kappa), P_m^{prev}(1-\tau))$. A detailed pseudo-code of the heuristic is provided in Algo. 2.

Strongest Signal-based Assignment with LED-first Approach (SSA-LED): This approach is a blend of the previous two approaches - the scanning procedure is LED-by-LED like *NUA* and the assignment is based on channel strength like *SSA-User*. For each LED m in the bulb, this approach checks whether there is any user inside it's coverage, either directly or via the mirror. We allocate $\min(P_m^{prev}(1+\tau), \bar{P})$ amount of source power when there is no or one user is covered by this LED. Now, if there are more than one user covered, we assign the current LED m to the user u_i with the strongest signal reception only if the number of the users covered by this LED is less than or equal to 3% of the total number of users. This is done to reduce the effect for interference when

Algorithm 2 Pseudo-code for *SSA-User* Heuristic Approach

$\boldsymbol{M} \leftarrow$ Number of LEDs, $\boldsymbol{U} \leftarrow$ Number of users
$\boldsymbol{P_1^{prev}}, \boldsymbol{P_2^{prev}}, \ldots \boldsymbol{P_M^{prev}} \leftarrow$ Allocated power to the LEDs from the LINEARIZED_MIRROR_DESIGN solution
$\boldsymbol{\tau} \leftarrow$ Allowed deviation from intermediate value of allocated LED power
for $\boldsymbol{j}$ = 1 to $\boldsymbol{U}$ **do**
  $\boldsymbol{cnt} \leftarrow$ Number of LEDs pointing towards the user $\boldsymbol{j}$
  if $\boldsymbol{cnt} \leq 1$ **then**
    if $\boldsymbol{cnt} == 1$ **then**
      Set $\boldsymbol{\epsilon_{ij}} \leftarrow 1$ $\{\boldsymbol{i}$ is the only LED pointing towards user $\boldsymbol{j}\}$
      Set $\boldsymbol{P_i} \leftarrow \min(\boldsymbol{P_i^{prev}} + \boldsymbol{\tau}, \bar{\boldsymbol{P}})$
    end if
  else
    $\boldsymbol{\kappa} \leftarrow 0,\ \boldsymbol{c_{max}} \leftarrow 0,\ \boldsymbol{c'_{max}} \leftarrow 0,\ \boldsymbol{cnt} \leftarrow 0$
    for $\boldsymbol{m}$ = 1 to $\boldsymbol{M}$ where $\boldsymbol{m}$ is an LED pointing towards user $\boldsymbol{j}$ **do**
      if $\boldsymbol{\epsilon_{mj}} == 1$ **then**
        if $\boldsymbol{H_{mj}} \geq \boldsymbol{c'_{max}}$ **then**
          Set $\boldsymbol{c'_{max}} \leftarrow \boldsymbol{H_{mj}}, \boldsymbol{cnt} \leftarrow \boldsymbol{cnt} + 1$
        end if
      else
        if $\boldsymbol{H_{mj}} \geq \boldsymbol{c_{max}}$ **then**
          Set $\boldsymbol{c_{max}} \leftarrow \boldsymbol{H_{mj}}, \boldsymbol{l} \leftarrow \boldsymbol{m}$
        end if
      end if
    end for
    if $\boldsymbol{c_{max}} > 0$ **then**
      Set $\boldsymbol{\kappa} \leftarrow \frac{\boldsymbol{c'_{max}}}{\boldsymbol{c_{max}}}, \boldsymbol{\epsilon_{lj}} \leftarrow 1$
      Set $\boldsymbol{P_l} \leftarrow \max(\boldsymbol{P_l^{prev}}(1-\boldsymbol{\kappa}), \boldsymbol{P_l^{prev}}(1-\boldsymbol{\tau}))$
    end if
  end if
end for

multiple users are being covered by the same LED. We give fraction of P_m^{prev} to the current LED with a ratio $\kappa = \frac{H_{mu_j}}{H_{mu_i}}$, where u_j is the user with the second strongest signal reception from the LED m. Thus the power allocated to LED m is $\max(P_m^{prev}(1-\kappa), P_m^{prev}(1-\tau))$. A detailed pseudo-code of the heuristic is provided in Algo. 3.

Each of the above described approaches has its own advantages and disadvantages. All the three heuristics iteratively go through the search space and try to find good settings for ϵ_{mu} and P_m in MAXMIN_THROUGHPUT. *NUA* and *SSA-LED* follow an LED-by-LED scanning approach, while *SSA-User* uses a user-by-user scanning approach. *NUA* has the simplest approach, although it is likely the worst-performing one which is elaborated further in Section IV. *SSA-User* is suitable for the scenarios where the users in the room are prioritized in some manner as it is a user-by-user approach which provides the best service to the user which is chosen first. But this is the most expensive approach considering the time complexity as many of the LEDs are needed to be examined multiple times if they cover more than one user. *SSA-LED* can be considered as a balance between *NUA* and *SSA-User* since it is less complex than *SSA-User* and obtains better performance than *NUA*. It also provides fairness to all the users in the system.

C. Complexity of the Heuristic Approaches

As mentioned earlier, the number of LEDs in the bulb is large, and trying to find the optimum LED-user associations

Algorithm 3 Pseudo code for *SSA-LED* Heuristic Approach

$\boldsymbol{M} \leftarrow$ Number of LEDs, $\boldsymbol{U} \leftarrow$ Number of users
$\boldsymbol{P_1^{prev}}$, $\boldsymbol{P_2^{prev}}$, ... $\boldsymbol{P_M^{prev}} \leftarrow$ Allocated power to the LEDs from the LINEARIZED_MIRROR_DESIGN solution
$\boldsymbol{\tau} \leftarrow$ Allowed deviation from intermediate value of allocated LED power
for $\boldsymbol{i}$ = 1 to $\boldsymbol{M}$ **do**
  $\boldsymbol{cnt} \leftarrow$ Number of users covered by LED $\boldsymbol{i}$
  if $\boldsymbol{cnt} \leq 1$ **then**
    if $\boldsymbol{cnt} == 1$ **then**
      Set $\boldsymbol{\epsilon_{ij}} \leftarrow 1$ $\{\boldsymbol{j}$ is the only user in the cone of LED $\boldsymbol{i}\}$
    end if
    Set $\boldsymbol{P_i} \leftarrow \min(\boldsymbol{P_i^{prev}} + \boldsymbol{\tau}, \bar{\boldsymbol{P}})$
  else
    if $\boldsymbol{cnt} > 0.03\,\boldsymbol{U}$ **then**
      $\boldsymbol{u_1} \leftarrow$ User with the strongest signal reception from LED $\boldsymbol{i}$
      $\boldsymbol{u_2} \leftarrow$ User with the second strongest signal reception from LED $\boldsymbol{i}$
      Set $\boldsymbol{\kappa} \leftarrow \frac{\boldsymbol{H_{mu_2}}}{\boldsymbol{H_{mu_1}}}$, $\boldsymbol{\epsilon_{iu_1}} \leftarrow 1$
      Set $\boldsymbol{P_i} \leftarrow \max(\boldsymbol{P_i^{prev}}(1-\boldsymbol{\kappa}), \boldsymbol{P_i^{prev}}(1-\boldsymbol{\tau}))$
    end if
  end if
end for

through exhaustive search is practically infeasible since the users can change their positions at any moment. Since any number of LEDs can be theoretically assigned to a particular user, a huge number of LED-user assignment combinations is possible for each set of user coordinates. Thus, the necessity of low complexity heuristic algorithms arises. The proposed low complexity heuristic solutions to the communication problem do not have a problem of convergence as all of them are single pass solutions. *NUA* and *SSA-LED* goes through each LED one by one, and *SSA-User* goes through each user one by one to assign LEDs to the users which can obtain better throughput considering different priorities. As these heuristic approaches are capable to solve the communication problem in a single pass, they can make it practically feasible to solve the problem on the fly when the users are moving around. Complexity of our proposed heuristic algorithms in the previous section are described below.

We are assuming M total LEDs and U total users in our problem. In both *NUA* and *SSA-LED*, we check each of the LEDs to allocate source power and assign it to a user if needed. This effective runtime of checking this is $O(M)$. Calculating the channel values for all users will take $O(MU)$ time which is the most dominant component, so the overall runtime for both *NUA* and *SSA-LED* is $O(MU)$.

For *SSA-User*, we take an user-by-user approach, and there may be cases when there is a conflict while assigning an LED to a particular user. In the worst case, runtime of this will be $O(M^2)$ when but on average this will be $O(M \log M)$ as this situation is similar as the Quick Sort algorithm. Combining this with the running time $O(MU)$ to calculate the channel values, we find the overall time complexity of the *SSA-User* approach to be $O(M(U + \log M))$.

TABLE II: Simulation Parameters

Parameter	Value
Room Size	$6m \times 6m \times 3m$
Radius of the hemispherical bulb, R	$40cm$
Number of LEDs on the bulb, M	391
Radius of an LED transmitter, r_t	$1.5cm$
Divergence angle of the LEDs, θ_d	30^o
Maximum transmit power of the LEDs, $\bar{P}$	$0.1W$
Area of a PD receiver*, r_r	$5cm^2$
Area of a sensing point, r_s	$10cm^2$
Number of users, U	$2-12$
Number of sensing points, N	100
Visibility, V	$0.5km$
Optical signal wavelength, λ	$650nm$
AWGN spectral density, N_0	$2.5 \times 10^{-20} W/Hz$
Modulation bandwidth, B	$20MHz$
Minimum uniformity, μ	0.7
Minimum illumination, ϕ_2	400 lux
Maximum illumination, ϕ_1	600 lux

*We assume that an array of PDs is used to attain a large receiver area.

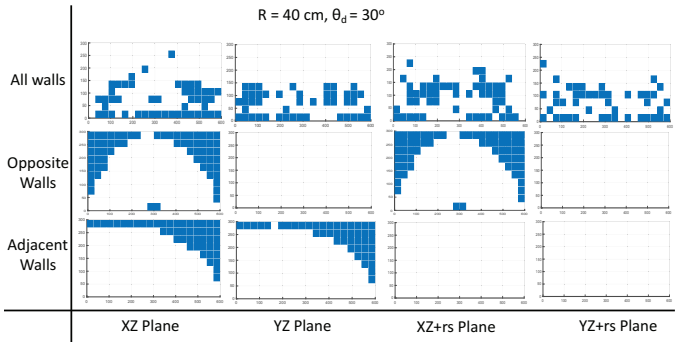

Fig. 7: Mirror placement heatmaps in four walls for different bulb radiuses and divergence angles.

IV. Simulation Results

In this section, we provide simulation results to study the performance of our MEMD VLC system model. Our aim is to make comparison between the three heuristics we proposed in terms of the *minimum throughput* and the *average throughput* of the system. To compare our proposed methods (*NUA*, *SSA-LED*, and *SSA-User*), we use the same input parameters for all of them. We randomly place the users on the room floor with their receiver's FOV normal looking towards the ceiling. We report the average of the minimum throughout , average throughput and illumination uniformity results among these randomly generated cases. To gain confidence in our results, we repeated the simulation experiments 100 times for all the results. We show the 95% confidence interval for the average throughput outputs as well.

We use white LEDs with luminous efficacy $\alpha_0 = 169$ lumen/watt [36]. The default values of the remaining input parameters used in our simulations are given in Table II. For placing LEDs on the bulb, we followed the method in Section II. In particular, for a bulb with R = 40cm radius, we place M = 391 LEDs on 20 layers with $k_{1..20}$ = [1, 6, 12, 15, 19, 26, 30, 37, 43, 33, 30, 28, 25, 21, 16, 13, 11, 10, 9, 6].

A. Placement of Mirrors

We solve the design problem in (18) using different mirror placement approaches for different scenarios. For $R = 40cm$ and $\theta_d = 30^o$, we solve the design problem considering three separate approaches : Mirror placement on 1) two adjacent walls, 2) two opposite walls and 3) all four walls. We define the four walls as XZ, YZ, $XZ + rs$ (the plane parallel with XZ-plane) and $YZ + rs$ (the plane parallel with YZ-plane) planes, where rs can be denoted as the room floor size. The mirror placement heatmaps from each of these scenarios are shown in Fig. 7. We can see that when we let the optimizer place mirrors on all four walls, it is difficult to establish any concrete pattern from the heatmaps although there are some similarities in placing the mirrors at lower altitudes. This happens because when the optimizer considers the sensing points near the corners of the room, there are several options to choose a mirror location from either of the two adjacent walls sharing the corner, and since there is no particular rule to do that, the mirrors are chosen randomly from those possible locations which could yield similar performance in terms of illumination level and uniformity, thus breaking the symmetry in the heatmaps. This is not the case when we allow the optimizer to place mirrors in two opposite walls as they do not share any corner, so we can see the same pattern of mirror placement in those two walls. Even in the case of two adjacent walls, the mirror placement follows the same pattern as the optimizer can avoid placing the mirror on the sides of the two walls which share the same corner and place most of the mirrors of the sides which do not share the same corner, as illustrated in the figure.

B. Performance Comparison among Mirror Placement Approaches

We compare the performance in terms of minimum throughput, average throughput and average illumination for the different mirror placement approaches. We also solve the design problem with no mirror placement at all to determine how much improvement is possible with mirror placement. The key findings are shown in Figs. 8 and 9. As the solution of the design problem is focused on optimizing the illumination, we see a noticeable three-fold improvement in average illumination level when mirror placement is applied, with the approach of placement in all walls having the most improvement aligning with our expectations. We can see up to four-fold increase in the average throughput values when comparing the four-wall case with the no mirror case. This fact indicates that placing mirror in all four walls can create more interference/noise for some users but at the same time they also provide better signal strength to most of the users resulting better average throughput. Adjacent and opposite walls cases also yield a solid improvement in both of average throughput and illumination level.

An interesting insight revealed from the results is that placement of mirrors can be detrimental in terms of fairness. As shown in Figs. 8 and 9, although the without mirror case suffers from low illumination and average throughput performances, it achieves better minimum throughput compared to the with-mirror cases. This is due to that the without mirror case does not solve the design problem as the design problem tackles the placement of mirrors. On the other hand, the with-mirror solutions first solve the design problem and decide which grid locations to place the mirrors on the walls, and then, they solve the communication problem. Once the mirrors are placed, the solution space for the communication problem is constrained with the existence of the mirrors. Since the design stage places the mirrors for more uniform illumination and ignores the throughput, the placement of the mirrors limits the solution space for the communication problem. Even though we expect the mirrors to help the overall performance (both in terms of illumination uniformity and average throughput), we observe that for some users the throughput can suffer, which explains the low minimum throughput for the with-mirror cases in Figs. 8(a) and 9(a). This is, in essence, a result of our two-staged approach to the overall MirrorVLC problem. Monolithic methods, exploring the solutions for both stages at the same time, may find better outcomes. Further, our heuristics for the NP-hard communication problem are only able to find sub-optimal solutions, and there may still be solutions attaining minimum throughput similar to (or better than) the without-mirror case.

Overall, these comparisons provide valuable insights with regard to VLC network design. Since a much higher level of illumination can be obtained on average from the same number of LEDs, either of the three mirror placement approaches can be seen as beneficial. A trade-off between system performance and ease of mirror deployment can be observed among the approaches. Among the three approaches, placing mirror in all four walls is the one which can yield maximum performance improvement in terms of illumination. In terms of average throughput, all the three approaches demonstrate better performance compared to the no mirror approach. However, in terms of the ease of mirror deployment, placing mirrors in the opposite walls is arguably the preferable approach as the mirror placement pattern is such that most of the chosen mirror grids are connected to each other - in that case the group of connected mirrors can be placed as a larger mirror - making the deployment easier. In rest of the simulations, we use the four walls approach to obtain intermediate results from the design problem which are used to solve the communication problem.

C. Comparison between NUA, SSA-LED, and SSA-User

We compare our proposed heuristic approaches for solving the communication problem, *NUA*, *SSA-LED* and *SSA-User*. We compare both minimum and average throughput among the users with average illumination level across the sensing points from 2 to 12 users for these three approaches. As seen in Fig. 10, minimum and average throughput decreases for all three approaches with increased number of users. The NUA heuristic approach, which is based on assigning the LED to the user closest to its beam, definitely suffers more in terms of average throughput because of the interference compared to *SSA-LED* or *SSA-User*. For *SSA-User*, minimum throughput has lower value compared to *NUA* because this approach highly prioritizes the users chosen first for LED assignments, which

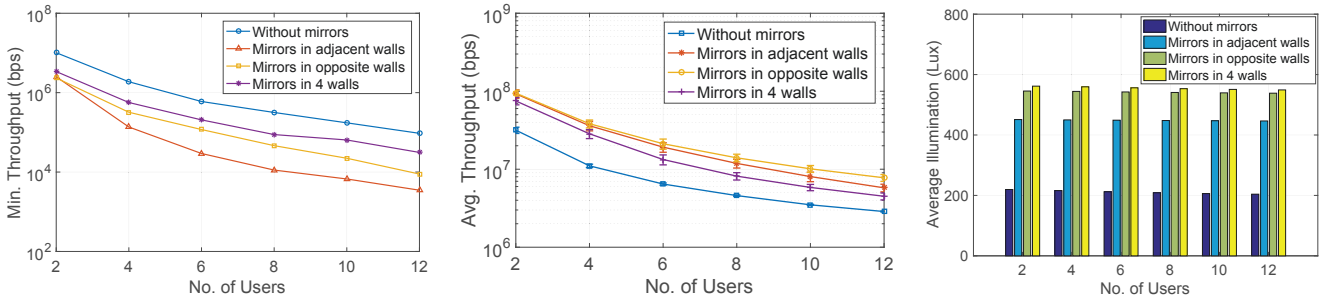

(a) Minimum throughput vs. No. of users. (b) Average throughput vs. No. of users. (c) Average illumination vs. No. of users.

Fig. 8: Comparison between different mirror placement approaches for *NUA* with $M = 391$ and $\theta_d = 30^o$.

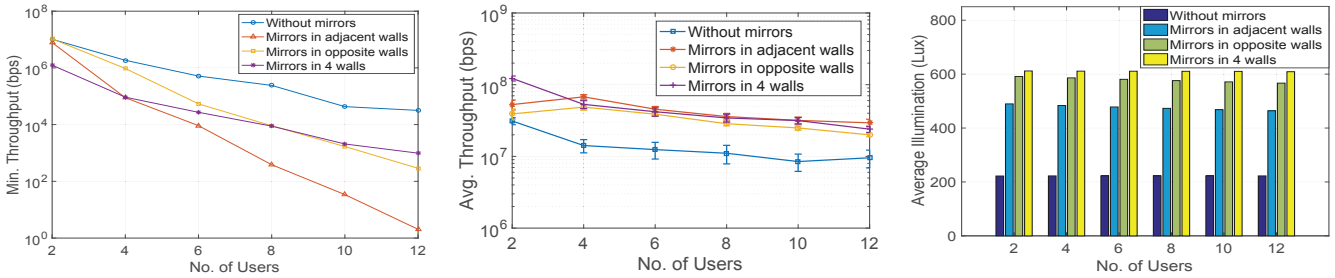

(a) Minimum throughput vs. No. of users. (b) Average throughput vs. No. of users. (c) Average illumination vs. No. of users.

Fig. 9: Comparison between different mirror placement approaches for *SSA-User* with $M = 391$ and $\theta_d = 30^o$.

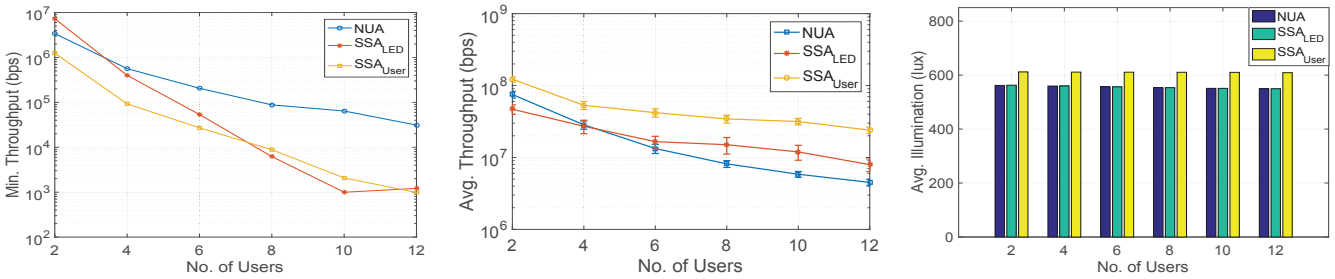

(a) Minimum throughput vs. No. of users. (b) Average throughput vs. No. of users. (c) Average illumination vs. No. of users.

Fig. 10: Comparison between *NUA*, *SSA-LED* and *SSA-User* with $M = 391$ and $\theta_d = 30^o$.

largely affects the users chosen at the end. *SSA-LED* also has lower values compared to *NUA*, as the restriction of assignment for some of the LEDs leads some users to starvation. But the average throughput is better for *SSA-LED* than *NUA* as that restriction ensures a considerable decline in interference as well. *SSA-User* does even better in terms of the average throughput as the high quality service provided to the users assigned first comprehensively overpowers the low quality service provided to the users in the end. In Fig. 10(c), we can see that the average illumination remains steady for all heuristics with increasing number of users since changes in LED source power allocation for these heuristics are not substantial enough to have any adverse effect on the overall illumination level.

D. Effect of Divergence Angle

For each of our proposed heuristics, we plot minimum and average throughput with average illumination in the room for different divergence angles when there are six users in total, shown in Fig. 11. With larger divergence angles, the LED beams get larger, thus there are more chances of a particular user to get coverage of an LED, but at the same time the chance of interference increases too. Changes in divergence angle does not seem have much impact on minimum throughput for *SSA-LED* and *SSA-User* because of the randomness in user locations. Looking at the average throughput, *SSA-LED* and *SSA-User* handle the interference better than *NUA* for increasing divergence angles as shown in Fig. 11(b). Average illumination level is not hampered much with either heuristic in this case as well.

It can be observed that the curves in Fig. 11 is not very smooth for some cases. The reason behind this is, in our two-stage problem solution approach, the intermediate results from the design problem are used to obtain the solution of the communication problem and the final output. For each of the different cases, these intermediate results from the design problem solution are different, the effect of which can be

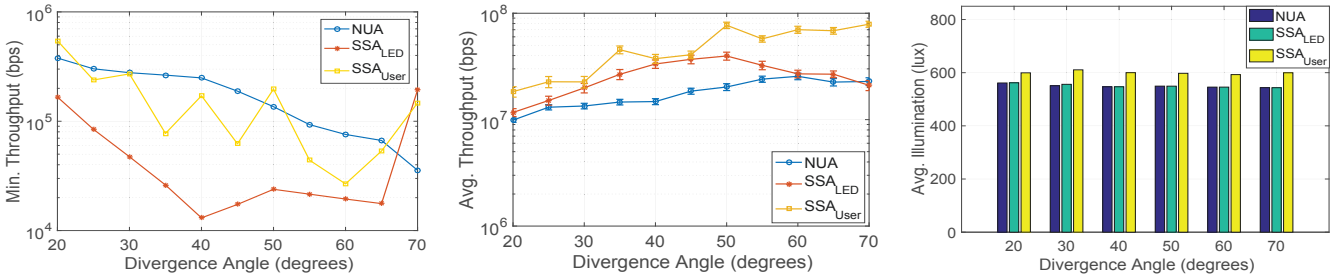

(a) Minimum throughput vs. Divergence angle. (b) Average throughput vs. Divergence angle. (c) Average illumination vs. Divergence angle.

Fig. 11: Comparison between *NUA*, *SSA-LED* and *SSA-User* for different divergence angles with 6 users. $M = 391$ and $R = 40cm$.

seen in the final output. To demonstrate this, we have added a comparison graph in Fig. 12, where we compare the average throughput curve of SSA-User from Fig. 11(b), which includes the mirror allocations from the design stage, against the average throughput curve where we obtained the final results for all divergence angles using the same intermediate result for a particular divergence angle (70^o in this case). It can be observed that the latter curve, which does not include the contribution of the mirrors from the design stage, is much smoother as it does not have the effect of different intermediate results from the design problem.

Fig. 13 shows the effect of the error in CSI on the system performance. We vary the variance of the CSI error σ_e^2 between -200 dB and -20 dB. Note that $\sigma_e^2 = 0$ corresponds to to the perfect CSI scenario). We plot the achievable throughput versus the error variance σ_e^2 with $R = 40$, $M = 391$ and $\theta_d = 30^o$ for algorithm $SSA - User$ with 6 users. We notice that the scheme performance is highly affected by the increase of the CSI error. For example, with $\sigma_e^2 = -140$ dB, the throughput reduces by around 25 times by having imperfect CSI instead of perfect CSI.

V. Related Work

One of the main challenging tasks in a multi-element VLC architecture is how to assign group of transmitters (i.e., LEDs) to each receiver, a.k.a. LED-user association, in the room at the same time, i.e., serving all users in the room simultaneously and taking the illumination requirements into consideration. There have been several studies to find optimum LED arrangements in MEMD VLC systems to obtain different goals like evenly distributed lighting [37], reducing SINR fluctuation [11], improving SINR while maintaining a certain illumination requirement [12], using cooperative beamforming to optimize total system throughput [38], minimizing of the number of LEDs to satisfy illumination constraints while maximizing of the average quality-of-experience of users [39], and allocating resources in a multi-cell and multi-user scenario based on data rate maximization and fairness criterion in the network [34].

Beyond the LED-user association problem, multi-element VLC networks require attention to the resource allocation among many potential links in the system. Even though the resource allocation problem in wireless communications has a long history, VLC or hybrid RF/VLC networks present unique challenges. In a comprehensive approach, [40] used deep learning to jointly optimize the bandwidth and power allocation while solving the LED-user association problem when a single RF access point is complemented with many VLC access points. In a similar vein, [41] iteratively solved the LED-user association and bandwidth allocation problems using federated learning for RF/VLC networks. Notably, [42] formulated the problem of jointly optimizing user associate and power allocation in a three-tier RF/VLC network as a combinatorial problem, proved that it is NP hard, and offered low-cost heuristic solutions using matching theory. Further, [43] used convex optimization to maximize energy efficiency of RF/VLC networks while satisfying constraints of minimum rate per user by dimming control within a maximum transmit power budget.

Recent efforts also explored the resource allocation trade-offs involved in non-orthogonal multiple access (NOMA) VLC channels. For example, [44] studied the optimization of power allocation to NOMA VLC links by trading off aggregate transmission rate and fairness among users, and presented how the optimization impacts the coverage probability of users. Impact of backscattering due to reflections from the environment [45] was considered into the channel performance in a NOMA VLC system. Error rate performance of NOMA under different modulation schemes for an SEMD VLC system was studied [46]. Interaction between dimming control and coding scheme being used by the LED transmitters is also explored within the context of multi-element VLC [47]. Following a more static design, [48] studied the design of constellations of LEDs using different colors and collectively applying color-shift keying as the modulation scheme. Within the context of multi-element VLC systems, energy consumption and transfer were given consideration as well. The work presented in [49] proposed an optimization problem aiming to minimize the total power consumption of multiple LEDs while satisfying certain data rate quality-of-service. Recently, simultaneous lightwave information and power transfer using non-linear energy harvesting model was proposed to extend the battery life of the VLC receivers [50].

Our work is different from these works for mainly two reasons: 1) Optimizing MEMD VLC system design with highly directional LEDs, and 2) Employing mirrors in the walls to use

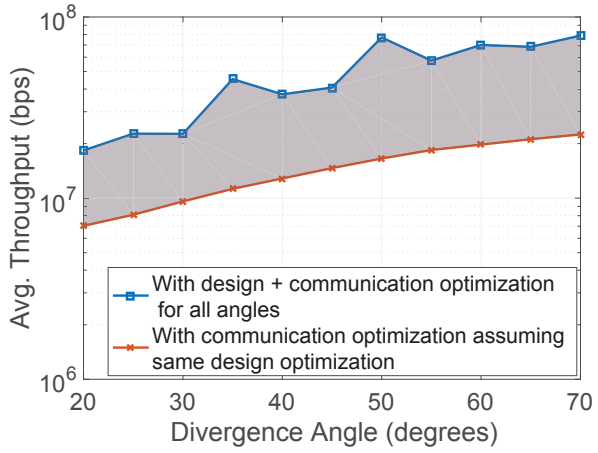

Fig. 12: Comparison between using same vs. different design optimizations.

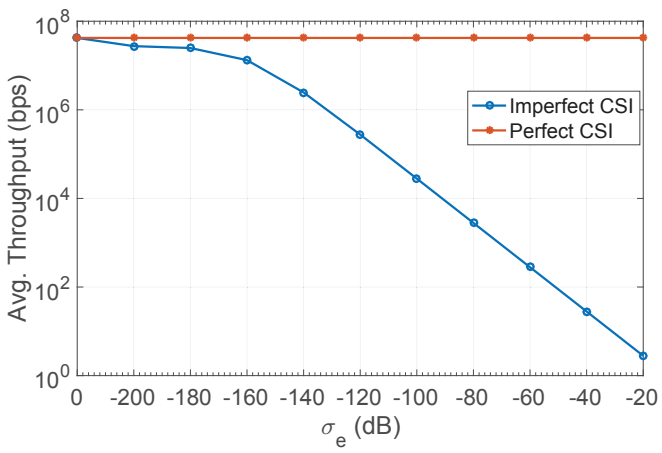

Fig. 13: Achieved throughput as a function of σ_e^2 under imperfect CSI.

the nLoS component of the VLC channel looking to improve both SINR and illumination uniformity. There have not been much research on using mirrors in optimizing VLC networks. In [21], deployment of a double-sized mirror between the receiver photo-detectors is utilized to propose a mirror diversity receiver design which can help in reduction of the channel correlation by attaining two things - obstructing the reception of the light from a particular direction and enhancing the channel gain from another direction. The authors claim this mirror diversity receiver to be an encouraging approach to boost the performance of the VLC system, but the use and benefit from the mirror placement approach are still very limited unlike our work - where we have explored optimum mirror placement in all walls of the room, facilitating to broaden the scope of improvement for both lighting distribution and the SINR.

VI. Summary and Future Work

In this paper, we have explored a novel mirror employment approach for performance improvement for an MEMD VLC system. In order to maximize the average throughput and illumination, we have formulated an optimization problem to obtain optimum mirror placement, power allocation and LED-user association. As the problem is NP-complete, we have proposed a two-stage solution of the optimization problem. As a part of the solution of the first stage, we have introduced several mirror placement approaches and analyzed their performance. To deal with heavy computation complexity in the second stage with the communication problem, we have presented multiple heuristic approaches to solve it with a detailed analysis on their performance. We have shown that up to threefold increase in average illumination and fourfold increase in average throughput can be achieved using a mirror placement approach.

In light of our proposed mirror placement approach, many promising future works are possible in the realm of indoor MEMD VLC networks. For example, it is worth exploring different mirror sizes and shapes which might yield further improvement in throughput or illumination level. For the communication problem, other heuristic algorithms may be explored to attain results that are closer to the optimal solution. It would also be worth observing how the proposed algorithms and mirror placement approaches perform with different system parameters (e.g., room shape, shape of the bulb) and whether there are any relationship between them. In our work, we considered a single bulb in a standard size room. Designing a MEMD VLC system for a much larger indoor environment with multiple such bulb is definitely a challenging and promising direction. In case of larger room size, increasing the bulb radius is a viable option which will be able to accommodate more LEDs and cover the larger room area. Multiple bulbs can also be deployed as another alternative where the optimum placement of these bulbs on the room ceiling to ensure minimum interference would be the key. For different bulb shapes, placement of LEDs in the bulb for better coverage could be another interesting item to explore.

Further, since we have assumed a multi-datastream communication system, each LED is assumed to have the capability to transmit in parallel. This effectively means that the electrical data signal for each LED can be band-limited to 20MHz. However, implementing a controller and driver circuit for many LEDs such that each one of them can transmit a different datastream will be a challenge. Future work is necessary to explore the trade-off between more flexibility in controlling each LED's data signal and the effective minimum bandwidth necessary for the electrical circuity to drive the LEDs in the bulb system.

We took a two-staged approach to the overall Mirror VLC problem. Several future works can be done to enhance the performance. It is possible to iterate between the design and communication stages multiple times to search for a better overall solution. Yet, such iterations will require convergence guarantees between the design and communication solutions. This could potentially allow the final solution to be closer to the optimum in terms of maximizing the minimum throughput, but that would also require mirrors to be more flexibly placed on the walls. In this direction, use intelligent reflecting mirrors

with the capability to reflect the light in specific directions dynamically may be utilized. To reduce the need for flexible mirrors, machine learning can be used to estimate the user count and distribution in the room and use these statistical information as an input to the design problem.

Energy efficiency, i.e., minimizing the ratio of energy consumption over the data rate, has been a well-studied aspect of radio communications and is an increasingly important aspect of VLC. Even though ample light power is available due to the illumination goals of VLC, reducing energy consumption is becoming more important as the number of elements in a VLC system is increasing [49]. In this paper, we have introduced the concept of using mirrors for VLC and focused on maximizing the minimum data rate for all users while keeping the illumination uniformity above an acceptable level. Our approach indirectly addresses the energy consumption by putting a limit on the transmit power of each LED. Proper consideration of energy efficiency in MirrorVLC is needed by reformulating our objective functions, particularly in MAXMIN_THROUGHPUT, which will pose an interesting problem to study.

REFERENCES

[1] L. Feng, H. Yang, R. Q. Hu, and J. Wang, "Mmwave and VLC-based indoor channel models in 5G wireless networks," *IEEE Wireless Communications*, vol. 25, no. 5, pp. 70–77, Aug. 2018.

[2] D. Wu, Z. Ghassemlooy, H. LeMinh, S. Rajbhandari, and Y. S. Kavian, "Power distribution and Q-factor analysis of diffuse cellular indoor visible light communication systems," in *Proc. of the 16th European Conference on Networks and Optical Communications, Newcastle upon Tyne, UK*, July 2011, pp. 28–31.

[3] A. Tsiatmas, F. M. J. Willems, and S. Baggen, "Optimum diversity combining techniques for VLC systems," in *Proc. of the IEEE IEEE Global Communications Conference Workshops, (GC Wkshps), Austin, TX, USA*, Austin, TX, Dec. 2014.

[4] M. Ijaz, D. Tsonev, A. Stavridis, A. Younis, J. J. D. McKendry, E. Gu, M. D. Dawson, S. Videv, and H. Haas, "Optical spatial modulation OFDM using micro LEDs," in *Proc. of the 48th Asilomar Conference on Signals, Systems and Computers, Pacific Grove, CA, USA*, Nov. 2014, pp. 1734–1738.

[5] A. F. Aziz, O. A. Aly, and U. S. Mohammed, "High efficiency modulation technique for visible light communication (VLC)," in *Proc. of the 36th National Radio Science Conference (NRSC), Port Said, Egypt*, June 2019, pp. 100–107.

[6] A. Nuwanpriya, S.-W. Ho, and C. S. Chen, "Angle diversity receiver for indoor MIMO VLC," in *Proc. of the IEEE IEEE Global Communications Conference Workshops (GC Wkshps), Austin, TX, USA*, Dec. 2014.

[7] A. H. Azhar, T. Tran, and D. O'Brien, "A Gigabit/s indoor wireless transmission using MIMO-OFDM visible-light communications," *IEEE Photonics Technology Letters*, vol. 25, no. 2, pp. 171–174, Jan. 2013.

[8] S. I. Mushfique, P. Palathingal, Y. S. Eroglu, M. Yuksel, I. Guvenc, and N. Pala, "A software-defined multi-element VLC architecture," *IEEE Communications Magazine*, vol. 56, no. 2, pp. 196–203, 2018.

[9] M. S. Mossaad, S. Hranilovic, and L. Lampe, "Visible light communications using OFDM and multiple LEDs," *IEEE Transactions on Communications*, vol. 63, no. 11, pp. 4304–4313, Nov. 2015.

[10] S. I. Mushfique and M. Yuksel, "Optimal multi-element vlc bulb design with power and lighting quality constraints," in *Proc. of the 3rd ACM Workshop on Visible Light Communication Systems (VLCS), New York, USA*, Oct. 2016, pp. 7–12.

[11] Z. Wang, C. Yu, W.-D. Zhong, J. Chen, and W. Chen, "Performance of a novel LED lamp arrangement to reduce SNR fluctuation for multi-user visible light communication systems," *Optics express*, vol. 20, no. 4, pp. 4564–4573, Jan. 2012.

[12] J.-H. Liu, Q. Li, and X.-Y. Zhang, "Cellular coverage optimization for indoor visible light communication and illumination networks," *Journal of Communications*, vol. 9, no. 11, pp. 891–898, Nov. 2014.

[13] P. F. Mmbaga, J. Thompson, and H. Haas, "Performance analysis of indoor diffuse VLC MIMO channels using angular diversity detectors," *IEEE Journal of Lightwave Technology*, vol. 34, no. 4, pp. 1254–1266, Feb. 2016.

[14] A. M. Abdelhady, O. Amin, A. Chaaban, and M.-S. Alouini, "Resource allocation for outdoor visible light communications with energy harvesting capabilities," in *Proc. of the IEEE Global Communications Conference Workshops (GLOBECOM Workshop), Singapore, Singapore*, Dec. 2017, pp. 1–6.

[15] G. B. Prince and T. D. C. Little, "On the performance gains of cooperative transmission concepts in intensity modulated direct detection visible light communication networks, valencia, spain," in *Proc. of the 6th IEEE International Conference on Wireless and Mobile Communications*, Sept. 2010, pp. 297–302.

[16] P. M. Butala, H. Elgala, and T. D. Little, "SVD-VLC: A novel capacity maximizing VLC MIMO system architecture under illumination constraints," in *Proc. of the IEEE Global Communication Conference Workshops (GLOBECOM Workshops), Atlanta, GA, USA*, Dec. 2013, pp. 1087–1092.

[17] S. Ibne Mushfique, A. Alsharoa, and M. Yuksel, "Optimization of sinr and illumination uniformity in multi-led multi-datastream vlc networks," *IEEE Transactions on Cognitive Communications and Networking*, vol. 6, no. 3, pp. 1108–1121, Feb. 2020.

[18] Z. Chen, D. Tsonev, and H. Haas, "Improving SINR in indoor cellular VLC networks," in *Proc. of the IEEE International Conference on Communications (ICC), Sydney, Australia*, June 2014, pp. 3383–3388.

[19] A. Tsiatmas, F. M. J. Willems, and S. Baggen, "Optimum diversity combining techniques for VLC systems," in *Proc. of the IEEE Global Commnication Conference Workshops (GLOBECOM Workshop), Austin, TX, USA*, Dec. 2014, pp. 456–461.

[20] Z. Ghassemlooy, W. Popoola, and S. Rajbhandari, *Optical wireless communications: system and channel modelling with Matlab®*. CRC press, 2019.

[21] K.-H. Park, H. M. Oubei, W. G. Alheadary, B. S. Ooi, and M.-S. Alouini, "A novel mirror-aided non-imaging receiver for indoor 2 x 2 MIMO-visible light communication systems," *IEEE Transactions on Wireless Communications*, vol. 16, no. 9, pp. 5630–5643, June 2017.

[22] A. Al Hammadi, P. C. Sofotasios, S. Muhaidat, M. Al-Qutayri, and H. Elgala, "Non-orthogonal multiple access for hybrid VLC-RF networks with imperfect channel state information," *IEEE Transactions on Vehicular Technology*, vol. 70, no. 1, pp. 398–411, Jan. 2021.

[23] A. Alsharoa, H. Ghazzai, and M.-S. Alouini, "Efficient multiple antenna–relay selection algorithms for MIMO unidirectional–bidirectional cognitive relay networks," *Transactions on Emerging Telecommunications Technologies*, vol. 27, no. 2, pp. 170–183.

[24] N. Lee, O. Simeone, and J. Kang, "The effect of imperfect channel knowledge on a MIMO system with interference," *IEEE Transactions on Communications*, vol. 60, no. 8, pp. 2221–2229, Aug. 2012.

[25] I. Standardization, "Lighting for work places part 1: Indoor," *International Commission on illumination*, Aug. 2002.

[26] Bax music Netherlands. (2017) Lite gear LED PAR 30 7W lamp WW Edison 45gn, Accessed June 2021. [Online]. Available: https://www.bax-shop.nl/producten-uit-assortiment/lite-gear-led-par-30-7w-lamp-ww-edison-45g.

[27] Y. S. Eroglu, I. Güvenç, A. Sahin, Y. Yapici, N. Pala, and M. Yuksel, "Multi-element VLC networks: LED assignment, power control, and optimum combining," *IEEE Journal on Selected Areas in Communications*, vol. 36, no. 1, Jan. 2018.

[28] A. Alsharoa, H. Ghazzai, E. Yaacoub, M.-S. Alouini, and A. E. Kamal, "Joint bandwidth and power allocation for MIMO two-way relays-assisted overlay cognitive radio systems," *IEEE Transactions on Cognitive Communications and Networking*, vol. 1, no. 4, pp. 383–393, Oct. 2015.

[29] T. Omar, Z. Abichar, A. E. Kamal, J. M. Chang, and M. A. Alnuem, "Fault-tolerant small cells locations planning in 4G/5G heterogeneous wireless networks," *IEEE Transactions on Vehicular Technology*, vol. 66, no. 6, pp. 5269–5283, June 2017.

[30] A. Alsharoa, X. Zhang, D. Qiao, and A. Kamal, "An energy-efficient relaying scheme for internet of things communications," in *Proc. of the IEEE International Conference on Communications (ICC), Kansas City, MO, USA*, May 2018, pp. 1–6.

[31] Gurobi, "Gurobi optimizer reference manual," 2016. Available [online]: http://www.gurobi.com/.

[32] CVX, "Mixed-integer support in CVX 2.0," 2012. Available [online]: http://cvxr.com/news/2012/08/midcp/.

[33] X. Bi, J. Zhang, Y. Wang, and P. Viswanath, "Fairness improvement of maximum C/I scheduler by dumb antennas in slow fading channel," in

Proc. of the 72nd IEEE Vehicular Technology Conference (Fall), Ottawa, Canada, Sept. 2010, pp. 1–4.
[34] M. Hammouda, A. M. Vegni, J. Peissig, and M. Biagi, "Resource allocation in a multi-color DS-OCDMA VLC cellular architecture," *Optics Express*, vol. 26, no. 5, pp. 5940–5961, Feb. 2018.
[35] Y. Song and G. Li, "Cross-layer optimization for OFDM wireless networks-Part I: Theoretical framework," *IEEE Transactions on Wireless Communications*, vol. 4, no. 2, pp. 614–624, Apr. 2005.
[36] P. M. Pattison, M. Hansen, and J. Y. Tsao, "LED lighting efficacy: Status and directions," *Elsevier Comptes Rendus Physique*, vol. 19, no. 3, pp. 134–145, 2018.
[37] A. Burton, H. Le Minh, Z. Ghasemlooy, and S. Rajbhandari, "A study of LED lumination uniformity with mobility for visible light communications," in *Proc. of the International Workshop on Optical Wireless Communications (IWOW), Pisa, Italy*, Oct. 2012, pp. 1–3.
[38] N. Cen, N. Dave, E. Demirors, Z. Guan, and T. Melodia, "LiBeam: Throughput-optimal cooperative beamforming for indoor visible light networks," in *Proc. of the IEEE Joint Conference: INFOCOM, IEEE Computer and Communications Societies*, June 2019, pp. 1972–1980.
[39] J. Li, X. Bao, and W. Zhang, "LED adaptive deployment optimization in indoor VLC networks," *China Communications*, vol. 18, no. 6, pp. 201–213, 2021.
[40] S. Shrivastava, B. Chen, C. Chen, H. Wang, and M. Dai, "Deep Q-network learning based downlink resource allocation for hybrid rf/vlc systems," *IEEE Access*, vol. 8, pp. 149 412–149 434, 2020.
[41] C. Liu, C. Guo, Y. Yang, M. Chen, H. V. Poor, and S. Cui, "Optimization of user selection and bandwidth allocation for federated learning in VLC/RF systems," in *Proceedings of IEEE Wireless Communications and Networking Conference (WCNC)*, 2021, pp. 1–6.
[42] S. Aboagye, T. M. N. Ngatched, O. A. Dobre, and A. Ibrahim, "Joint access point assignment and power allocation in multi-tier hybrid RF/VLC hetnets," *IEEE Transactions on Wireless Communications*, 2021.
[43] S. Ma, F. Zhang, H. Li, F. Zhou, M.-S. Alouini, and S. Li, "Aggregated VLC-RF Systems: achievable rates, optimal power allocation, and energy efficiency," *IEEE Transactions on Wireless Communications*, vol. 19, no. 11, pp. 7265–7278, 2020.
[44] Z. Dong, T. Shang, Q. Li, and T. Tang, "Differential evolution-based optimal power allocation scheme for NOMA-VLC systems," *Optics Express*, vol. 28, no. 15, pp. 21 627–21 640, July 2020.
[45] D. Shi, L. Shi, and X. Zhang, "A joint backscatter and VLC-NOMA communication scheme for B5G/6G umMTC system," in *Proceedings of IEEE International Symposium on Broadband Multimedia Systems and Broadcasting*, August 2021.
[46] X. Liu, Z. Chen, Y. Wang, F. Zhou, Y. Luo, and R. Q. Hu, "BER analysis of NOMA-enabled visible light communication systems with different modulations," *IEEE Transactions on Vehicular Technology*, vol. 68, no. 11, pp. 10 807–10 821, Sept. 2019.
[47] Y. Yang, Y. Yang, C. Wang, C. Guo, and H. Xia, "Hybrid dimming scheme based on transmit antenna selection and precoding for MU MC VLC system," in *Proceedings of IEEE Global Communications Conference (GLOBECOM)*, 2020, pp. 1–6.
[48] D.-F. Zhang, H.-Y. Yu, and Y.-J. Zhu, "A multi-user joint constellation design of color-shift keying for vlc downlink broadcast channels," *Optics Communications*, vol. 473, p. 126001, 2020.
[49] S. I. Mushfique, A. Dey, A. Alsharoa, and M. Yuksel, "Resource optimization in visible light communication for internet of things," in *Proc. of the IEEE International Symposium on Local and Metropolitan Area Networks (LANMAN), Paris, France*, July 2019, pp. 1–6.
[50] X. Liu, Z. Chen, Y. Wang, F. Zhou, S. Ma, and R. Q. Hu, "Secure beamforming designs in miso visible light communication networks with slipt," in *GLOBECOM 2020 - 2020 IEEE Global Communications Conference*, 2020, pp. 1–6.

Sifat Ibne Mushfique received the B.Sc. degree in electrical and electronic engineering from the Bangladesh University of Engineering and Technology in 2011. He completed the Ph.D. degree with the Department of Computer Engineering, University of Central Florida, Orlando, FL, USA. He is currently working at Intel Corporation as a Software Engineer in the Technology Development Analytics and Technology Automation (TD ATA) group.

Ahmad Alsharoa (S'14, M'18, SM'19) was born in Irbid, Jordan. He received the PhD degree from Iowa State University, USA, in May 2017. He is currently an assistant professor in the Electrical and Computer Engineering department at Missouri University of Science and Technology (Missouri S&T). Since 2021, he has been on the Editorial Board of the IEEE Wireless Communications Letters and the Frontiers in Communications and Networks journal. His current research interests include: smart systems, mobile wireless networks, high-altitude and satellite communications, edge computing, optical sensing and communications, reconfigurable intelligent surfaces, and green communications.

Murat Yuksel (SM'11) is a Professor and the Interim Chair at the ECE Department of the University of Central Florida (UCF), Orlando, FL. Prior to UCF, he was a faculty member at the CSE Department of the University of Nevada, Reno, NV. From 2002 to 2006, he was a member of Adjunct Faculty and a Postdoctoral Associate at the ECSE Department of Rensselaer Polytechnic Institute (RPI), Troy, NY. He received his B.S. degree in computer engineering from Ege University, Izmir, Turkey in 1996, and M.S. and Ph.D. degrees in computer science from RPI in 1999 and 2002, respectively. He worked as a software engineer at Pepperdata, and a visiting researcher at AT&T Labs and Los Alamos National Lab. His research interests are in the areas of networked, wireless, and computer systems. He has been on the editorial boards of Computer Networks and IEEE Networking Letters. He has published more than 200 papers at peer-reviewed journals and conferences, and is a co-recipient of three Best Paper, one Best Paper Runner-up, and one Best Demo Awards. He is a senior member of IEEE, senior and life member of ACM, and was a member of Sigma Xi.